

Non-Hermitian Anharmonicity Induces Single-Photon EmissionAnael Ben-Asher^{✉,*}, Antonio I. Fernández-Domínguez[✉], and Johannes Feist[✉]*Departamento de Física Teórica de la Materia Condensada and Condensed Matter Physics Center (IFIMAC),
Universidad Autónoma de Madrid, E28049 Madrid, Spain*

(Received 10 December 2022; accepted 22 May 2023; published 16 June 2023)

Single-photon sources are in high demand for quantum information applications. A paradigmatic way to achieve single-photon emission is through anharmonicity in the energy levels, such that the absorption of a single photon from a coherent drive shifts the system out of resonance and prevents absorption of a second one. We identify a novel mechanism for single-photon emission through non-Hermitian anharmonicity, i.e., anharmonicity in the losses instead of in the energy levels. We demonstrate the mechanism in two types of systems, including a feasible setup consisting of a hybrid metallodielectric cavity weakly coupled to a two-level emitter, and show that it induces high-purity single-photon emission at high repetition rates.

DOI: [10.1103/PhysRevLett.130.243601](https://doi.org/10.1103/PhysRevLett.130.243601)

The generation and manipulation of nonclassical light are essential for light-based quantum information technologies [1]. Nonclassical light is characterized by photons that are correlated with each other, and therefore, their arrival times are dependent. The likelihood to detect coincident photons is usually quantified by the normalized high-order correlation functions at zero delay, $g_{\tau=0}^{(n \geq 2)}$ [2]. While $g_{\tau}^{(n)} = 1$ characterizes a coherent source of classical light with a Poissonian distribution of the photon arrival times, $g_{\tau=0}^{(n=2)} < 1$ characterizes a sub-Poissonian distribution associated with quantum light. When $g_{\tau=0}^{(n)} \ll 1$, the source can essentially only emit a single photon at a time. Such single-photon devices play a vital role in secure communications [3,4], quantum computing [5–8], quantum metrology [9–11], and quantum sensing [12].

Single-photon emission can be generated by emitters that behave like two-level systems to a good approximation, such as atoms [13], nitrogen-vacancy centers in diamonds [14], and quantum dots [15]. While these inherently nonlinear systems offer a straightforward approach for single-photon emission, they have limitations in efficiency, emission rates, coherence time, and scalability [14,16,17]. As an alternative, cavity modes, which couple efficiently to light and are highly tunable, can potentially be used to achieve bright photon emission at high rates. However, they are inherently linear due to their bosonic nature, such that single-photon emission can only be achieved through physical mechanisms inducing an effective nonlinearity [18]. In this Letter, we describe a novel mechanism for generating efficient single-photon emission at high rates using cavity modes.

A prominent mechanism for the generation of single photons using cavity modes is the so-called photon blockade (PB, also known as conventional antibunching) [19–21] phenomenon observed across various platforms, e.g., in cavity quantum electrodynamical (QED) [19,20]

and optomechanical [22,23] systems. This mechanism is traditionally interpreted in terms of the eigenstates of the undriven Hermitian Hamiltonian, which describes the effect of the coherent coupling of the system components but does not describe the modification of these dynamics due to losses. The anharmonicity of these eigenstates, i.e., the fact that the energy required to absorb one photon is different from the energy required to absorb a subsequent photon, induces the photon blockade effect. In contrast, the novel mechanism introduced in this Letter is based on the anharmonicity of the eigenstates of the effective undriven non-Hermitian (NH) Hamiltonian arising from the Lindblad master equation for open quantum systems [24,25]. It becomes efficient when there is a significant difference in the losses (encoded in the imaginary parts of the NH eigenenergies) of the singly and doubly excited states of the system. Thus, we show that the effective NH Hamiltonian not only provides a mathematically convenient description including the effect of losses, but naturally points the way toward a non-Hermitian photon blockade (NHPB) mechanism. In this aspect, it is similar to phenomena such as exceptional points and parity-time symmetry that have attracted much attention in the last decade [26–35], and also arise naturally from a NH description.

Hermitian PB is difficult to realize in lossy systems, as the anharmonicity has to be larger than the linewidths (that are determined by the loss rates) of the system eigenstates [21], which is only achieved in the strong-coupling regime of cavity QED systems. In contrast, NHPB is not limited by the linewidths but instead exploits their possibly large values and operates in the weak-coupling regime of cavity QED systems, as we show below. The NHPB mechanism is thus expected to have less stringent experimental requirements than the Hermitian PB for the realization of an efficient single-photon source. Note that another antibunching mechanism, the destructive interference mechanism

(also known as unconventional antibunching) [36–38] also usually operates in the weak-coupling regime; however, it suffers from severe limitations for single-photon generation [39].

We obtain a unified description of the PB phenomenon, which includes both the Hermitian and the NH mechanisms, using a perturbative approach to obtain a simple expression for the correlation functions under weak pumping by a continuous-wave source at frequency ω_L . The derivation details and the full expressions are given in the Supplemental Material [40]. In the common situation that only one eigenstate in each excitation manifold contributes significantly to the emission, the normalized zero-delay second-order correlation function $g_{\tau=0}^{(2)}$ is given by

$$g_{\tau=0}^{(2)}(\omega_L) \approx \left| \frac{\tilde{E}_{p_1} - \hbar\omega_L}{\frac{\tilde{E}_{p_2}}{2} - \hbar\omega_L} \right|^2 \frac{|(p_2|\hat{V}_p|p_1)|^2}{2|(p_1|\hat{V}_p|0)|^2} \times \frac{|(p_2|E_D^- E_D^- E_D^+ E_D^+|p_2)|}{2|(p_1|E_D^- E_D^+|p_1)|^2}, \quad (1)$$

where \hat{V}_p is the pumping operator that the external driving laser couples to, transformed into its rotating frame; E_D^- is the scattered far-field operator at the detector; $|0\rangle$ is the ground state; and $|p_1\rangle$, $|p_2\rangle$ are the relevant eigenstates of the NH laser-free Hamiltonian in its first- and second-excitation manifolds. Their complex eigenenergies $\tilde{E}_j = E_j - (i/2)\Gamma_j$, where j can be either p_1 or p_2 , encode both the energy position E_j and loss rate Γ_j . Note that for eigenstates of a NH Hamiltonian, the notation $|\dots\rangle$, $\langle\dots|$ rather than $|\dots\rangle$, $\langle\dots|$ is used to describe the right and left eigenstates [41].

The emergence of both Hermitian and non-Hermitian PB manifests itself in the first row of Eq. (1), which presents the ratio between the populations of $|p_2\rangle$ and $|p_1\rangle$. In particular, the first term of Eq. (1) can be strongly suppressed when there is nonlinearity in the complex plane, i.e., when $\tilde{E}_{p_1} \neq (\tilde{E}_{p_2}/2)$. Figure 1 shows a sketch of these two mechanisms: while the Hermitian PB in Fig. 1(a) stems from anharmonicity in the real axis $E_{p_1} \neq (E_{p_2}/2)$, the NHPB in Fig. 1(b) occurs even when $E_{p_1} = (E_{p_2}/2) = \hbar\omega_L$ and stems from the anharmonicity in the imaginary

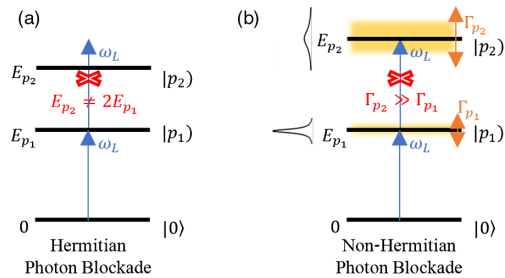


FIG. 1. Sketch of the two mechanisms for PB: (a) the Hermitian mechanism and (b) the NHPB mechanism introduced in this Letter.

part of the eigenenergies. When the decay rate of $|p_2\rangle$ is much larger than that of $|p_1\rangle$, i.e., when $\Gamma_{p_2} \gg \Gamma_{p_1}$, as illustrated in Fig. 1(b), the state $|p_2\rangle$ is effectively eliminated from the dynamics such that the absorption of a second photon is prevented and $g_{\tau=0}^{(2)}(\omega_L)$ is strongly suppressed. Note that the first term of Eq. (1) is the ratio between two Lorentzian functions centered at E_{p_1} and $E_{p_2}/2$ and whose widths are Γ_{p_1} and $\Gamma_{p_2}/2$, respectively. These Lorentzian functions are also depicted in Fig. 1(b). They represent the energy-dependent densities of states that correspond to $|p_1\rangle$ and $|p_2\rangle$ in the real energy spectrum and originate from their NH character [41]. This observation provides a physical explanation for the NHPB, revealing that the absorption of subsequent photons is suppressed due to a smaller density of states at twice the laser frequency than at the laser frequency itself.

As described above, realizing the NHPB mechanism requires a setup with a nonlinear behavior in losses. Specifically, the narrowest accessible eigenstates, i.e., those with the lowest losses, in each excitation manifold of the laser-free system are the relevant $|p_1\rangle$ and $|p_2\rangle$ that should obey $\Gamma_{p_1} \ll \Gamma_{p_2}$ to induce it. This points toward a way to design single-photon sources by engineering the loss of the levels in the system, instead of designing a specific energetic structure and trying to minimize losses as the Hermitian PB suggests. In the following, we theoretically demonstrate this concept and present the implementation of the NHPB mechanism through the engineering of losses by tailoring the coherent coupling between different modes with a given loss within the effective NH laser-free Hamiltonian framework. Note that this loss-engineering approach differs from actively designing the operators in the Lindblad master equation to modify the system's interaction with the environment states [42–45]. We present two examples where the necessary nonlinearity is induced by different effects. The first example is a proof-of-principle model with nonlinear coupling between linear elements that facilitates analytical analysis, while the second example presents a realistic system of a hybrid metalodielectric cavity interacting with a two-level emitter (TLE) in which the nonlinearity is due to linear coupling to a nonlinear system: a TLE.

The first example is a prototypical NH Hamiltonian describing second-harmonic generation [46],

$$\hat{H}_0 = \tilde{\omega}_a a^\dagger a + \tilde{\omega}_b b^\dagger b + g(a^\dagger b^2 + (b^\dagger)^2 a), \quad (2)$$

where a (a^\dagger) and b (b^\dagger) are the annihilation (creation) operators of two bosonic modes, $\tilde{\omega}_a = 2\omega_b - (i/2)\gamma_a$ and $\tilde{\omega}_b = \omega_b - (i/2)\gamma_b$ are their complex energies, and g is the quadratic coupling strength between them. Note that we have assumed that the real parts of the energies are exactly on two-photon resonance. This simple Hamiltonian can be analyzed analytically without any restriction to just a few eigenstates. In particular, when weakly pumping the b

mode ($\hat{V}_p = b^\dagger + b$) on resonance ($\omega_L = \omega_b$), and detecting its emission ($E_D^- \propto b^\dagger$), the intensity I and the normalized zero-delay second-order correlation function $g_{\tau=0}^{(2)}$ are given by

$$I(\omega_L = \omega_b) \propto \frac{4}{\gamma_b^2}, \quad g_{\tau=0}^{(2)}(\omega_L = \omega_b) = \frac{1}{(1 + \eta)^2}, \quad (3)$$

where $\eta = (4g^2/\gamma_a\gamma_b)$ is the cooperativity parameter for the two modes [47]. $g_{\tau=0}^{(2)}(\omega_L = \omega_b)$ vanishes when $\eta \gg 1$. While large cooperativity can be obtained either through a large g , through a small γ_a , or through a small γ_b , the latter limit leads to the highest intensity and thus the most efficient single-photon emission. This limit corresponds exactly to the NHPB mechanism, while the limits of large g and small γ_a correspond to the Hermitian PB and the destructive interference mechanism, respectively. In the NHPB limit, the accessible first-excitation eigenstate $|p_1\rangle$, that is the pure b mode with $\Gamma_{p_1} = \gamma_b$, is narrow. The second-excitation eigenstates, however, which arise from the interaction between the singly excited mode a and the doubly excited mode b , are much broader when $\gamma_b \ll \gamma_a$. In particular, when the coupling is weak ($g < (\gamma_a/2\sqrt{2})$), the decay rate of the narrowest state $|p_2\rangle$ is given by $\Gamma_{p_2} \approx 2\gamma_b(1 + \eta)$. Thus, we obtain $g_{\tau=0}^{(2)}(\omega_L = \omega_b) \approx (2\Gamma_{p_1}/\Gamma_{p_2})^2$, demonstrating the manifestation of the NHPB mechanism. In addition, to emphasize that the low two-photon emission given by $g_{\tau=0}^{(2)}(\omega_L = \omega_b)$ indicates the low two-photon absorption characterizing the NHPB, we note that the upconversion efficiency of two absorbed photons with frequency ω_b to one emitted photon with frequency $2\omega_b$, given by $\Phi_{\text{up}} = [\eta/(\eta + \gamma_a/\gamma_b)]$ (see Ref. [40] for details), is very small in the NHPB limit.

The Hamiltonian in Eq. (2) can, e.g., describe a mechanical oscillator (mode b) located exactly in the middle of a Fabry-Pérot cavity (mode a), when the optical mode is strongly driven by a laser (see Refs. [48–50]). Since commonly the mechanical decay rate is much smaller than the optical one [48–50], the NHPB induces single-phonon emission in such a system. For example, for $(\gamma_b/\gamma_a) = 10^{-3}$ and $g = (\gamma_a/10)$, the cooperativity is $\eta = 40$. Consequently, $g_{\tau=0}^{(2)}(\omega_L = \omega_b) \approx 6 \times 10^{-3}$ [Eq. (3)], showing strong antibunching. Note that adiabatic elimination of the mode a in Eq. (2) leads to a single oscillator with a nonlinear loss. Single-phonon emission in such a system has been demonstrated in Ref. [51].

The second example we discuss is a feasible cavity-QED-like setup involving the linear coupling of a TLE to bosonic (cavity) modes. In order to generate the anharmonicity in the complex plane that induces the NHPB, two bosonic modes with different losses are required. Hybrid metallodielectric cavities, incorporating a narrow photonic mode and a broad plasmonic mode, provide an excellent

platform that fits this requirement. These cavities have attracted much attention lately, both theoretically [52–55] and experimentally [56–58], since they combine the merits of low-loss microcavities with highly localized plasmons, thus yielding new functionalities. Very recent works [59–62] have studied the photon statistics of a hybrid cavity coupled to a TLE and showed that it can present strong antibunching. These works related the antibunching to the destructive interference mechanism [59–61], and/or used large coupling strengths or energy detuning to induce the Hermitian PB mechanism [60–62]. In contrast, we here demonstrate that NHPB in such a system can lead to efficient single-photon emission without requiring large coupling strengths or energy detunings.

The NH Hamiltonian that describes the coupling between a TLE and two optical modes (e.g., a Fabry-Pérot mode and a plasmonic mode) can be written as

$$\hat{H}_0 = \left(\omega_e - i\frac{\gamma_e}{2} \right) \sigma_+ \sigma_- + \sum_{n=1,2} \left[\left(\omega_n - i\frac{\gamma_n}{2} \right) a_n^\dagger a_n + g_n (\sigma_+ a_n + a_n^\dagger \sigma_-) \right] + d(a_1^\dagger a_2 + a_2^\dagger a_1). \quad (4)$$

Here, σ_- (σ_+) and a_n (a_n^\dagger) are the annihilation (creation) operators of the TLE and the two optical modes, respectively; ω_e , ω_n and γ_e , γ_n are respectively their energies and decay rates; g_1 , g_2 are the coupling strengths between the TLE and each optical mode; and d is the coupling strength between the two optical modes originating from the interaction between the Fabry-Pérot electric field and the plasmonic dipole moment. Note that due to the non-Hermiticity of the system and the fact that the Hermitian and anti-Hermitian parts of the effective Hamiltonian do not commute, diagonalizing the Hermitian part to decouple the two optical modes would yield dissipative interactions. Consequently, there is no equivalent system of uncoupled bosonic modes that provides the same dynamics [63,64]. In the following, we show the importance of the coupling d in inducing the NHPB mechanism. Without loss of generality, we assign index 1 to the narrow (Fabry-Pérot) mode and index 2 to the broad (plasmonic) mode, such that $\gamma_2 \gg \gamma_1$. In addition, we consider $\gamma_e \ll \gamma_{1,2}$, which describes a good emitter at low temperatures (e.g., see Ref. [65]). Figure 2 depicts an illustration of the system.

The NHPB mechanism is induced in the system above by the decoupling of the Fabry-Pérot mode and emitter from the plasmonic mode occurring when g_2 , $d \gg g_1, \gamma_e, \gamma_1$ [40]. This decoupling is only present in the first-excitation manifold, forming a very narrow $|p_1\rangle$. The state $|p_1\rangle$ resembles the dark state formed when several emitters interact with a cavity [66]. However, $|p_1\rangle$ is optically accessible by pumping the Fabry-Pérot mode and detecting its emission, such that $\hat{V}_p = a_1^\dagger + a_1$ and $E_D^- \propto a_1^\dagger$. These operators describe a system configuration in which its

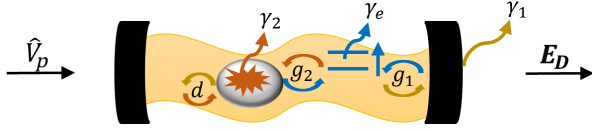


FIG. 2. Scheme of a hybrid metallodielectric cavity interacting with a TLE. The parameters characterizing the system are sketched. \hat{V}_p and E_D describe the pumping of the Fabry-Pérot mode and the detection of its emission, respectively.

driving from and leakage into free space is mediated by the mirrors of the Fabry-Pérot cavity, as is presented in Fig. 2. Reference [62] has discussed the formation of a very narrow $|p_1\rangle$ in a hybrid cavity interacting with a TLE and presented its role in enhancing the efficiency of the single-photon emission occurring due to the Hermitian PB mechanism. We here show that by engineering the decay rate of the narrowest state in the second-excitation manifold, $|p_2\rangle$, the very narrow $|p_1\rangle$ can be used to induce the NHPB mechanism.

The decay rate of $|p_2\rangle$ is engineered by controlling its plasmonic component. The plasmonic mode participates in $|p_2\rangle$ through its coupling d to the Fabry-Pérot mode. Figure 3 studies the single-photon emission due to the NHPB mechanism with respect to d when $\gamma_1 = 10^{-3}\gamma_2$, $\gamma_e = 10^{-5}\gamma_2$, $g_1 = 0$, $g_2 = (\gamma_2/15)$, and $\omega_e = \omega_1 = \omega_2$. In Fig. 3(a), $g_{\tau=0}^{(2)}$ is shown as a function of the laser detuning $\Delta\omega_L = \omega_e - \omega_L$ and the coupling d , when pumping the Fabry-Pérot mode and detecting its emission. Note that, although not shown, the intensity reaches its maximum for $\Delta\omega_L = 0$ because the coupling strengths are sufficiently small not to induce Rabi splitting. The observed antibunching stems from the NHPB mechanism, i.e., from the anharmonicity in the imaginary part of the eigenenergies. This anharmonicity is presented in Fig. 3(b), which depicts the decay rates Γ_j of the first (red) and second (black) excitation eigenstates, normalized by the excitation number $q = 1, 2$, as a function of d . The decay rates of $|p_1\rangle$ and $|p_2\rangle$ are in thicker lines. Figure 3(c) plots the plasmonic components of $|p_1\rangle$ (dark red line) and of $|p_2\rangle$ (gray line), given by $|(p_1|a_2^\dagger a_2|p_1)|$ and $|(p_2|a_2^\dagger a_2|p_2)|$, respectively, as a function of d . While the component of the plasmon in $|p_1\rangle$ is kept very small, consistent with its decoupling from $|p_1\rangle$, its component in $|p_2\rangle$ increases with larger d . When it reaches the ratio γ_1/γ_2 [dashed horizontal line in Fig. 3(c)], the decay rate of $|p_2\rangle$ becomes significantly larger than that of $|p_1\rangle$ [Fig. 3(b)], inducing the emission of single photons [Fig. 3(a)].

Similarly to the previous example, $g_{\tau=0}^{(2)}$ can be expressed as a function of the cooperativity between the two optical modes $\eta = (4d^2/\gamma_1\gamma_2)$:

$$g_{\tau=0}^{(2)}(\omega_L = \omega_e) \approx \frac{1}{\eta^2} \left[\frac{g_2^2}{d^2} + 2 + 4 \left(\frac{g_2}{\gamma_2} \right)^2 \left(\frac{g_2^2}{d^2} - 1 \right) \right]^2, \quad (5)$$

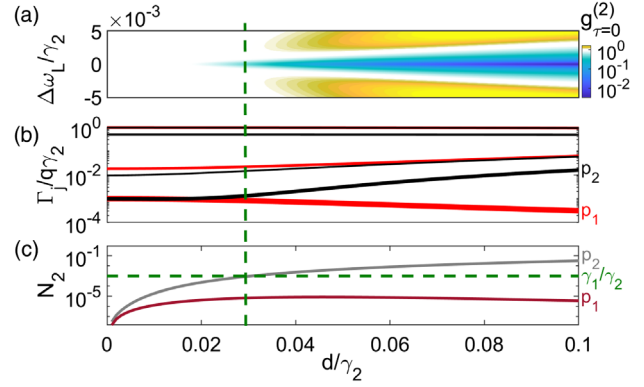


FIG. 3. (a) $g_{\tau=0}^{(2)}$ as a function of $\Delta\omega_L$, and d . (b) Γ_j/q of the first (red, $q = 1$) and the second (black, $q = 2$) excitation eigenstates and (c) $N_2^{p_1} = |(p_1|a_2^\dagger a_2|p_1)|$ (dark red) and $N_2^{p_2} = |(p_2|a_2^\dagger a_2|p_2)|$ (gray) as a function of d .

showing that large η is required to achieve antibunching. Equation (5) is the second-order approximation for the analytical expression of $g_{\tau=0}^{(2)}(\omega_L = \omega_e)$ when $(\gamma_1/\gamma_2) \ll 1$ and $\gamma_e = 0$. Further investigation of the dependence of the results and their robustness with respect to the system parameters is presented in the Supplemental Material [40].

Finally, in Fig. 4, we analyze the validity of the approximations inherent to our analysis above. Figures 4(a) and 4(b) plot I and $g_{\tau=0}^{(2)}$, respectively, as a function of $\Delta\omega_L$ when $d = (\gamma_2/10)$ (and the other parameters are as in Fig. 3). In addition, since single-photon emission requires the suppression of all the high-order correlations $g_{\tau=0}^{(n)}$, we present in Fig. 4(c) the normalized zero-delay third-order correlation function $g_{\tau=0}^{(3)}$ as a function of $\Delta\omega_L$. The strong dip in Fig. 4(c) (solid line) demonstrates that the NHPB operates beyond second-order processes and suppresses multiphoton events. Moreover, the results support that the predicted antibunching

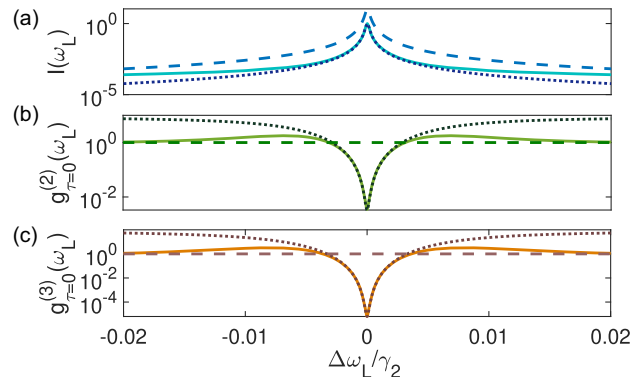


FIG. 4. (a) I , (b) $g_{\tau=0}^{(2)}$, and (c) $g_{\tau=0}^{(3)}$ as a function of $\Delta\omega_L$. The solid lines correspond to the full calculations [40], the dotted lines consider only the narrowest eigenstate in each excitation manifold, and the dashed lines were obtained when imposing $\Gamma_j = q\Gamma_{p_1}$ where q is the excitation number.

is related to the generalized PB phenomenon and not to the destructive interference effect [39]. To verify that the predicted antibunching can be well-understood in terms of just two system eigenstates, $|p_1\rangle$ and $|p_2\rangle$, as Eq. (1) does, we compare I , $g_{\tau=0}^{(2)}$ and $g_{\tau=0}^{(3)}$ obtained by including all system eigenstates (solid lines) with the values obtained only by the narrowest eigenstates in each manifold, $|p_1\rangle$, $|p_2\rangle$, and $|p_3\rangle$ (dotted lines). As can be seen, almost perfect agreement is achieved between the two cases in the vicinity of $\Delta\omega_L = 0$. Furthermore, we show that artificially setting all the eigenstates to have the same decay rate $\Gamma_j = q\Gamma_{p_1}$ (dashed lines) suppresses the antibunching completely. q is the excitation number, and Γ_{p_1} is the decay rate of $|p_1\rangle$. This suppression demonstrates that indeed the anharmonicity in the imaginary part of the eigenenergies, i.e., the NHPB mechanism, is the origin of the observed antibunching.

To conclude, we have theoretically proposed a novel mechanism for generating high-purity single-photon emission at high repetition rates. This mechanism stems from the difference in linewidth between the absorption of one photon and of two photons, and can be explained by the anharmonicity in the complex NH eigenenergy spectrum. Thus, the NHPB mechanism reveals an interesting interplay between non-Hermiticity of the system and quantum nonlinearity of the emitted light. Importantly, it provides a reliable route to single-photon emission even in the weak-coupling regime where couplings do not overcome losses. We have demonstrated the NHPB in two types of systems, including a feasible cavity-QED-like setup with realistic parameters, and showed that it indeed induces strong antibunching. Our findings open the door to the realization of new single-photon devices with potential applications in quantum information, communication, and metrology.

This work has been funded by the Spanish Ministry of Science, Innovation and Universities-Agencia Estatal de Investigación through Grants No. PID2021-126964OB-I00, No. PID2021-125894NB-I00, and No. CEX2018-000805-M (through the María de Maeztu program for Units of Excellence in R&D). We also acknowledge financial support from the Proyecto Sinérgico CAM 2020 Y2020/TCS-6545 (NanoQuCo-CM) of the Community of Madrid, from the European Research Council through Grant No. ERC-2016-StG-714870 and from the European Union's Horizon Europe Research and Innovation Programme through grant agreements No. 101070700 (MIRAQLS) and No. 101034324 (CIVIS3i).

*Corresponding author.

anael.benasher@uam.es

- [1] J. L. O'Brien, A. Furusawa, and J. Vučković, Photonic quantum technologies, *Nat. Photonics* **3**, 687 (2009).
 [2] R. Loudon, *The Quantum Theory of Light*, 1st ed. (Oxford University Press, Oxford, 1973).

- [3] N. Gisin, G. Ribordy, W. Tittel, and H. Zbinden, Quantum cryptography, *Rev. Mod. Phys.* **74**, 145 (2002).
 [4] V. Scarani, H. Bechmann-Pasquinucci, N.J. Cerf, M. Dušek, N. Lütkenhaus, and M. Peev, The security of practical quantum key distribution, *Rev. Mod. Phys.* **81**, 1301 (2009).
 [5] E. Knill, R. Laflamme, and G.J. Milburn, A scheme for efficient quantum computation with linear optics, *Nature (London)* **409**, 46 (2001).
 [6] P. Kok, W.J. Munro, K. Nemoto, T.C. Ralph, J.P. Dowling, and G.J. Milburn, Linear optical quantum computing with photonic qubits, *Rev. Mod. Phys.* **79**, 135 (2007).
 [7] D.E. Chang, A.S. Sørensen, E.A. Demler, and M.D. Lukin, A single-photon transistor using nanoscale surface plasmons, *Nat. Phys.* **3**, 807 (2007).
 [8] I. Shomroni, S. Rosenblum, Y. Lovsky, O. Bechler, G. Guendelman, and B. Dayan, All-optical routing of single photons by a one-atom switch controlled by a single photon, *Science* **345**, 903 (2014).
 [9] V. Giovannetti, S. Lloyd, and L. Maccone, Quantum Metrology, *Phys. Rev. Lett.* **96**, 010401 (2006).
 [10] V. Giovannetti, S. Lloyd, and L. Maccone, Advances in quantum metrology, *Nat. Photonics* **5**, 222 (2011).
 [11] C.J. Chunnillal, I.P. Degiovanni, S. Kück, I. Müller, and A.G. Sinclair, Metrology of single-photon sources and detectors: A review, *Opt. Eng.* **53**, 081910 (2014).
 [12] C.L. Degen, F. Reinhard, and P. Cappellaro, Quantum sensing, *Rev. Mod. Phys.* **89**, 035002 (2017).
 [13] B. Darquié, M.P. Jones, J. Dingjan, J. Beugnon, S. Bergamini, Y. Sortais, G. Messin, A. Browaeys, and P. Grangier, Controlled single-photon emission from a single trapped two-level atom, *Science* **309**, 454 (2005).
 [14] I. Aharonovich, S. Castelletto, D. Simpson, C.-H. Su, A. Greentree, and S. Praver, Diamond-based single-photon emitters, *Rep. Prog. Phys.* **74**, 076501 (2011).
 [15] J. Stachurski, S. Tamariz, G. Callsen, R. Butté, and N. Grandjean, Single photon emission and recombination dynamics in self-assembled GaN/AlN quantum dots, *Light Sci. Appl.* **11**, 114 (2022).
 [16] I. Aharonovich, D. Englund, and M. Toth, Solid-state single-photon emitters, *Nat. Photonics* **10**, 631 (2016).
 [17] J. Lee, V. Leong, D. Kalashnikov, J. Dai, A. Gandhi, and L.A. Krivitsky, Integrated single photon emitters, *AVS Quantum Sci.* **2**, 031701 (2020).
 [18] P. Lodahl, S. Mahmoodian, and S. Stobbe, Interfacing single photons and single quantum dots with photonic nanostructures, *Rev. Mod. Phys.* **87**, 347 (2015).
 [19] K.M. Birnbaum, A. Boca, R. Miller, A.D. Boozer, T.E. Northup, and H.J. Kimble, Photon blockade in an optical cavity with one trapped atom, *Nature (London)* **436**, 87 (2005).
 [20] J. Fink, M. Göppl, M. Baur, R. Bianchetti, P.J. Leek, A. Blais, and A. Wallraff, Climbing the Jaynes-Cummings ladder and observing its nonlinearity in a cavity QED system, *Nature (London)* **454**, 315 (2008).
 [21] A. Faraon, I. Fushman, D. Englund, N. Stoltz, P. Petroff, and J. Vučković, Coherent generation of non-classical light on a chip via photon-induced tunnelling and blockade, *Nat. Phys.* **4**, 859 (2008).

- [22] P. Rabl, Photon Blockade Effect in Optomechanical Systems, *Phys. Rev. Lett.* **107**, 063601 (2011).
- [23] K. Stannigel, P. Komar, S. J. M. Habraken, S. D. Bennett, M. D. Lukin, P. Zoller, and P. Rabl, Optomechanical Quantum Information Processing with Photons and Phonons, *Phys. Rev. Lett.* **109**, 013603 (2012).
- [24] P. M. Visser and G. Nienhuis, Solution of quantum master equations in terms of a non-Hermitian Hamiltonian, *Phys. Rev. A* **52**, 4727 (1995).
- [25] R. Sáez-Blázquez, J. Feist, F. J. García-Vidal, and A. I. Fernández-Domínguez, Photon statistics in collective strong coupling: Nanocavities and microcavities, *Phys. Rev. A* **98**, 013839 (2018).
- [26] M. Liertz, L. Ge, A. Cerjan, A. D. Stone, H. E. Türeci, and S. Rotter, Pump-Induced Exceptional Points in Lasers, *Phys. Rev. Lett.* **108**, 173901 (2012).
- [27] A. Regensburger, C. Bersch, M.-A. Miri, G. Onishchukov, D. N. Christodoulides, and U. Peschel, Parity–time synthetic photonic lattices, *Nature (London)* **488**, 167 (2012).
- [28] L. Chang, X. Jiang, S. Hua, C. Yang, J. Wen, L. Jiang, G. Li, G. Wang, and M. Xiao, Parity–time symmetry and variable optical isolation in active–passive-coupled microresonators, *Nat. Photonics* **8**, 524 (2014).
- [29] Y. Sun, W. Tan, H.-q. Li, J. Li, and H. Chen, Experimental Demonstration of a Coherent Perfect Absorber with PT Phase Transition, *Phys. Rev. Lett.* **112**, 143903 (2014).
- [30] J. Doppler, A. A. Mailybaev, J. Böhm, U. Kuhl, A. Girschik, F. Libisch, T. J. Milburn, P. Rabl, N. Moiseyev, and S. Rotter, Dynamically encircling an exceptional point for asymmetric mode switching, *Nature (London)* **537**, 76 (2016).
- [31] W. Chen, Ş. Kaya Özdemir, G. Zhao, J. Wiersig, and L. Yang, Exceptional points enhance sensing in an optical microcavity, *Nature (London)* **548**, 192 (2017).
- [32] J. Zhang, B. Peng, Ş. K. Özdemir, K. Pichler, D. O. Krimer, G. Zhao, F. Nori, Y.-x. Liu, S. Rotter, and L. Yang, A phonon laser operating at an exceptional point, *Nat. Photonics* **12**, 479 (2018).
- [33] C. Wang, X. Jiang, G. Zhao, M. Zhang, C. W. Hsu, B. Peng, A. D. Stone, L. Jiang, and L. Yang, Electromagnetically induced transparency at a chiral exceptional point, *Nat. Phys.* **16**, 334 (2020).
- [34] C. Wang, W. R. Sweeney, A. D. Stone, and L. Yang, Coherent perfect absorption at an exceptional point, *Science* **373**, 1261 (2021).
- [35] M. S. Ergoktas, S. Soleymani, N. Kakenov, K. Wang, T. B. Smith, G. Bakan, S. Balci, A. Principi, K. S. Novoselov, S. K. Ozdemir *et al.*, Topological engineering of terahertz light using electrically tunable exceptional point singularities, *Science* **376**, 184 (2022).
- [36] T. C. H. Liew and V. Savona, Single Photons from Coupled Quantum Modes, *Phys. Rev. Lett.* **104**, 183601 (2010).
- [37] M. Bamba, A. Imamoğlu, I. Carusotto, and C. Ciuti, Origin of strong photon antibunching in weakly nonlinear photonic molecules, *Phys. Rev. A* **83**, 021802(R) (2011).
- [38] A. Majumdar, M. Bajcsy, A. Rundquist, and J. Vučković, Loss-Enabled Sub-Poissonian Light Generation in a Bimodal Nanocavity, *Phys. Rev. Lett.* **108**, 183601 (2012).
- [39] E. Zubizarreta Casalengua, J. C. López Carreño, F. P. Laussy, and E. d. Valle, Conventional and unconventional photon statistics, *Laser Photonics Rev.* **14**, 1900279 (2020).
- [40] See Supplemental Material at <http://link.aps.org/supplemental/10.1103/PhysRevLett.130.243601> for the derivation of the correlation functions expressions, for the calculation of the upconversion efficiency in the first example and for further investigation of the dependence of the results in the second example (a hybrid cavity coupled to a TLE) with respect to the system parameters.
- [41] N. Moiseyev, *Non-Hermitian Quantum Mechanics* (Cambridge University Press, Cambridge, England, 2011).
- [42] J. F. Poyatos, J. I. Cirac, and P. Zoller, Quantum Reservoir Engineering with Laser Cooled Trapped Ions, *Phys. Rev. Lett.* **77**, 4728 (1996).
- [43] Z. Leghtas, S. Touzard, I. M. Pop, A. Kou, B. Vlastakis, A. Petrenko, K. M. Sliwa, A. Narla, S. Shankar, M. J. Hatridge *et al.*, Confining the state of light to a quantum manifold by engineered two-photon loss, *Science* **347**, 853 (2015).
- [44] A. Lingenfelter, D. Roberts, and A. Clerk, Unconditional fock state generation using arbitrarily weak photonic nonlinearities, *Sci. Adv.* **7**, eabj1916 (2021).
- [45] X. Su, J.-S. Tang, K. Xia, Nonlinear dissipation-induced photon blockade, *Phys. Rev. A* **106**, 063707 (2022).
- [46] C. Sanchez Muñoz, G. Frascella, and F. Schlawin, Quantum metrology of two-photon absorption, *Phys. Rev. Res.* **3**, 033250 (2021).
- [47] H. Tanji-Suzuki, I. D. Leroux, M. H. Schleier-Smith, M. Cetina, A. T. Grier, J. Simon, and V. Vuletić, Interaction between atomic ensembles and optical resonators: Classical description, in *Advances in Atomic, Molecular, and Optical Physics* (Elsevier, New York, 2011), Vol. 60, pp. 201–237.
- [48] H. Xie, G.-W. Lin, X. Chen, Z.-H. Chen, and X.-M. Lin, Single-photon nonlinearities in a strongly driven optomechanical system with quadratic coupling, *Phys. Rev. A* **93**, 063860 (2016).
- [49] Z.-Y. Li, G.-R. Jin, T.-S. Yin, and A. Chen, Two-phonon blockade in quadratically coupled optomechanical systems, *Photonics* **9**, 70 (2022).
- [50] H. Xie, C.-G. Liao, X. Shang, Z.-H. Chen, and X.-M. Lin, Optically induced phonon blockade in an optomechanical system with second-order nonlinearity, *Phys. Rev. A* **98**, 023819 (2018).
- [51] J. Li, C. Ding, and Y. Wu, Highly nonclassical phonon emission statistics through two-phonon loss of van der Pol oscillator, *J. Appl. Phys.* **128**, 234302 (2020).
- [52] X. Yang, A. Ishikawa, X. Yin, and X. Zhang, Hybrid photonic-plasmonic crystal nanocavities, *ACS Nano* **5**, 2831 (2011).
- [53] P. Peng, Y.-C. Liu, D. Xu, Q.-T. Cao, G. Lu, Q. Gong, Y.-F. Xiao, Enhancing Coherent Light-Matter Interactions through Microcavity-Engineered Plasmonic Resonances, *Phys. Rev. Lett.* **119**, 233901 (2017).
- [54] B. Gurlek, V. Sandoghdar, and D. Martín-Cano, Manipulation of quenching in nanoantenna–emitter systems enabled by external detuned cavities: A path to enhance strong-coupling, *ACS Photonics* **5**, 456 (2018).
- [55] N. Thakkar, M. T. Rea, K. C. Smith, K. D. Heylman, S. C. Quillin, K. A. Knapper, E. H. Horak, D. J. Masiello, and R. H. Goldsmith, Sculpting fano resonances to control

- photonic–plasmonic hybridization, *Nano Lett.* **17**, 6927 (2017).
- [56] M. Barth, S. Schietinger, S. Fischer, J. Becker, N. Nusse, T. Aichele, B. Lochel, C. Sonnichsen, and O. Benson, Nanoassembled plasmonic-photonic hybrid cavity for tailored light-matter coupling, *Nano Lett.* **10**, 891 (2010).
- [57] Y. Luo, M. Chamanzar, A. Apuzzo, R. Salas-Montiel, K. N. Nguyen, S. Blaize, and A. Adibi, On-chip hybrid photonic–plasmonic light concentrator for nanofocusing in an integrated silicon photonics platform, *Nano Lett.* **15**, 849 (2015).
- [58] S. Cui, X. Zhang, T.-l. Liu, J. Lee, D. Bracher, K. Ohno, D. Awschalom, and E. L. Hu, Hybrid plasmonic photonic crystal cavity for enhancing emission from near-surface nitrogen vacancy centers in diamond, *ACS Photonics* **2**, 465 (2015).
- [59] S. Shen, J. Li, and Y. Wu, Quantum statistics engineering in a hybrid nanoparticle-emitter-cavity system, *Phys. Rev. A* **105**, 063702 (2022).
- [60] Y.-W. Lu, J.-F. Liu, Z. Liao, and X.-H. Wang, Plasmonic-photonic cavity for high-efficiency single-photon blockade, *Sci. China Phys. Mech. Astron.* **64**, 274212 (2021).
- [61] Y.-W. Lu, J.-F. Liu, R. Li, Y. Wu, H. Tan, and Y. Li, Single-photon blockade in quasichiral atom–photon interaction: Simultaneous high purity and high efficiency, *New J. Phys.* **24**, 053029 (2022).
- [62] Y.-W. Lu, W.-J. Zhou, Y. Li, R. Li, J.-F. Liu, L. Wu, and H. Tan, Unveiling atom-photon quasi-bound states in hybrid plasmonic-photonic cavity, *Nanophotonics* **11**, 3307 (2022).
- [63] S. Franke, S. Hughes, M. K. Dezfouli, P. T. Kristensen, K. Busch, A. Knorr, and M. Richter, Quantization of Quasi-normal Modes for Open Cavities and Plasmonic Cavity Quantum Electrodynamics, *Phys. Rev. Lett.* **122**, 213901 (2019).
- [64] I. Medina, F. J. García-Vidal, A. I. Fernández-Domínguez, and J. Feist, Few-Mode Field Quantization of Arbitrary Electromagnetic Spectral Densities, *Phys. Rev. Lett.* **126**, 093601 (2021).
- [65] D. Wang, H. Kelkar, D. Martin-Cano, D. Rattenbacher, A. Shkarin, T. Utikal, S. Götzinger, and V. Sandoghdar, Turning a molecule into a coherent two-level quantum system, *Nat. Phys.* **15**, 483 (2019).
- [66] J. del Pino, J. Feist, and F. J. Garcia-Vidal, Quantum theory of collective strong coupling of molecular vibrations with a microcavity mode, *New J. Phys.* **17**, 053040 (2015).